

Measurement of the $B^0 - \bar{B}^0$ mixing parameter in DELPHI

DELPHI Collaboration

Abstract

A total of about 900.000 $Z^0 \rightarrow q\bar{q}$ decays have been analyzed to measure the $B^0 - \bar{B}^0$ mixing probability. Two different b tagging techniques have been used: events with two leptons and events with one lepton and one Λ . From a combination of the two methods the average mixing parameter, χ , was determined to be $(12.1 \pm 1.6(stat.) \pm 0.4(syst.) \pm 0.4(model))\%$.

(To be submitted to Physics Letters B)

P.Abreu²⁰, W.Adam⁷, T.Adye³⁷, E.Agasi³⁰, I.Ajinenko⁴², R.Aleksan³⁹, G.D.Alekseev¹⁴, P.P.Allport²¹,
 S.Almehed²³, F.M.L.Almeida⁴⁷, S.J.Alvsvaag⁴, U.Amaldi⁷, A.Andreazza²⁷, P.Antilogus²⁴, W-D.Apel¹⁵,
 R.J.Apsimon³⁷, Y.Arnoud³⁹, B.Åsman⁴⁴, J-E.Augustin¹⁸, A.Augustinus³⁰, P.Baillon⁷, P.Bambade¹⁸,
 F.Barao²⁰, R.Barate¹², G.Barbiellini⁴⁶, D.Y.Bardin¹⁴, G.J.Barker³⁴, A.Baroncelli⁴⁰, O.Barring⁷, J.A.Barrio²⁵,
 W.Bartl⁵⁰, M.J.Bates³⁷, M.Battaglia¹³, M.Baubillier²², K-H.Becks⁵², M.Begalli³⁶, P.Beilliere⁶, P.Beltran⁹,
 A.C.Benvenuti⁵, M.Berggren⁴¹, D.Bertrand², F.Bianchi⁴⁵, M.Bigi⁴⁵, M.S.Bilenky¹⁴, P.Billoir²², J.Bjarne²³,
 D.Bloch⁸, J.Blocki⁵¹, S.Blyth³⁴, V.Bocci³⁸, P.N.Bogolubov¹⁴, T.Bolognese³⁹, M.Bonesini²⁷, W.Bonivento²⁷,
 P.S.L.Booth²¹, G.Borisov⁴², C.Bosio⁴⁰, B.Bostjancic⁴³, S.Bosworth³⁴, O.Botner⁴⁸, B.Bouquet¹⁸,
 C.Bourdarios¹⁸, T.J.V.Bowcock²¹, M.Bozzo¹¹, S.Braibant², P.Branchini⁴⁰, K.D.Brand³⁵, R.A.Brenner¹³,
 H.Briand²², C.Bricman², L.Brillault²², R.C.A.Brown⁷, J-M.Brunet⁶, L.Bugge³², T.Buran³², A.Buys⁷,
 J.A.M.A.Buytaert⁷, M.Caccia²⁷, M.Calvi²⁷, A.J.Camacho Rozas⁴¹, R.Campion²¹, T.Camporesi⁷, V.Canale³⁸,
 K.Cankocak⁴⁴, F.Cao², F.Carena⁷, P.Carrilho⁴⁷, L.Carroll²¹, R.Cases⁴⁹, C.Caso¹¹, M.V.Castillo Gimenez⁴⁹,
 A.Cattai⁷, F.R.Cavallo⁵, L.Cerrito³⁸, V.Chabaud⁷, A.Chan¹, Ph.Charpentier⁷, J.Chauveau²², P.Checchia³⁵,
 G.A.Chelkov¹⁴, L.Chevalier³⁹, P.Chliapnikov⁴², V.Chorowicz²², J.T.M.Chrin⁴⁹, V.Cindro⁴³, P.Collins³⁴,
 J.L.Contreras¹⁸, R.Contri¹¹, E.Cortina⁴⁹, G.Cosme¹⁸, F.Couchot¹⁸, H.B.Crawley¹, D.Crennell³⁷, G.Crosetti¹¹,
 J.Cuevas Maestro³³, S.Czellar¹³, E.Dahl-Jensen²⁸, J.Dahm⁵², B.Dalmagne¹⁸, M.Dam³², G.Damgaard²⁸,
 E.Daubie², A.Daum¹⁵, P.D.Dauncey⁷, M.Davenport⁷, J.Davies²¹, W.Da Silva²², C.Defoix⁶, P.Delpierre²⁶,
 N.Demaria³⁴, A.De Angelis⁷, H.De Boeck², W.De Boer¹⁵, S.De Brabandere², C.De Clercq²,
 M.D.M.De Fez Laso⁴⁹, C.De La Vaissiere²², B.De Lotto⁴⁶, A.De Min²⁷, L.De Paula⁴⁷, H.Dijkstra⁷,
 L.Di Ciaccio³⁸, F.Djama⁸, J.Dolbeau⁶, M.Donszelmann⁷, K.Doroba⁵¹, M.Dracos⁸, J.Drees⁵², M.Dris³¹,
 Y.Dufour⁷, F.Dupont¹², D.Edsall¹, R.Ehret¹⁵, T.Ekelof⁴⁸, G.Ekspong⁴⁴, M.Elsing⁵², J-P.Engel⁸, N.Ershaidat²²,
 M.Espirito Santo²⁰, V.Falaleev⁴², D.Fassouliotis³¹, M.Feindt⁷, A.Fenyuk⁴², A.Ferrer⁴⁹, T.A.Filippas³¹,
 A.Firestone¹, H.Foeth⁷, E.Fokitis³¹, F.Fontanelli¹¹, F.Formenti⁷, J-L.Fousset²⁶, S.Francon²⁴, B.Franek³⁷,
 P.Frenkiel⁶, D.C.Fries¹⁵, A.G.Frodesen⁴, F.Fulda-Quenzer¹⁸, H.Furstenau⁷, J.Fuster⁷, D.Gamba⁴⁵,
 M.Gandelman¹⁷, C.Garcia⁴⁹, J.Garcia⁴¹, C.Gaspar⁷, U.Gasparini³⁵, Ph.Gavillet⁷, E.N.Gaziz³¹, D.Gele⁸,
 J-P.Gerber⁸, P.Giacomelli⁷, D.Gillespie⁷, R.Gokieli⁵¹, B.Golob⁴³, V.M.Golovatyuk¹⁴, J.J.Gomez Y Cadenas⁷,
 G.Gopal³⁷, L.Gorn¹, M.Gorski⁵¹, V.Gracco¹¹, F.Grad², E.Graziani⁴⁰, G.Grosdidier¹⁸, P.Gunnarsson⁴⁴,
 J.Guy³⁷, U.Haeding¹⁵, F.Hahn⁵², M.Hahn⁴⁴, S.Hahn⁵², S.Haider³⁰, Z.Hajduk¹⁶, A.Hakansson²³,
 A.Hallgren⁴⁸, K.Hamacher⁵², G.Hamel De Monchenault³⁹, W.Hao³⁰, F.J.Harris³⁴, V.Hedberg²³, R.Henriques²⁰,
 J.J.Hernandez⁴⁹, J.A.Hernando⁴⁹, P.Herquet², H.Herr⁷, T.L.Hessing²¹, E.Higon⁴⁹, H.J.Hilke⁷, T.S.Hill¹,
 S-O.Holmgren⁴⁴, P.J.Holt³⁴, D.Holthuisen³⁰, P.F.Honore⁶, M.Houlden²¹, J.Hrubic⁵⁰, K.Huet², K.Hultqvist⁴⁴,
 P.Ioannou³, P-S.Iversen⁴, J.N.Jackson²¹, R.Jacobsson⁴⁴, P.Jalocha¹⁶, G.Jarlskog²³, P.Jarry³⁹, B.Jean-Marie¹⁸,
 E.K.Johansson⁴⁴, M.Jonker⁷, L.Jonsson²³, P.Juillot⁸, M.Kaiser¹⁵, G.Kalmus³⁷, F.Kapusta²², M.Karlsson⁴⁴,
 E.Karvelas⁹, S.Katsanevas³, E.C.Katsoufis³¹, R.Keranen⁷, B.A.Khomenko¹⁴, N.N.Khovanski¹⁴, B.King²¹,
 N.J.Kjaer²⁸, H.Klein⁷, A.Klovning⁴, P.Kluit³⁰, A.Koch-Mehrin⁵², J.H.Koehne¹⁵, B.Koene³⁰, P.Kokkinias⁹,
 M.Koratzinos³², K.Korcyl¹⁶, A.V.Korytov¹⁴, V.Kostioukhine⁴², C.Kourkoumelis³, O.Kouznetsov¹⁴,
 P.H.Kramer⁵², M.Krammer⁵⁰, C.Kreuter¹⁵, J.Krolkowski⁵¹, I.Kronkvist²³, W.Krupinski¹⁶, K.Kulka⁴⁸,
 K.Kurvinen¹³, C.Lacasta⁴⁹, C.Lambropoulos⁹, J.W.Lamsa¹, L.Lanceri⁴⁶, P.Langefeld⁵², V.Lapin⁴², I.Last²¹,
 J-P.Laugier³⁹, R.Lauhakangas¹³, G.Leder⁵⁰, F.Ledroit¹², R.Leitner²⁹, Y.Lemoigne³⁹, J.Lemonne², G.Lenzen⁵²,
 V.Lepeltier¹⁸, T.Lesiak¹⁶, J.M.Levy⁸, E.Lieb⁵², D.Liko⁵⁰, R.Lindner⁵², A.Lipniacka¹⁸, I.Lippi³⁵, B.Loerstad²³,
 M.Lokajicek¹⁰, J.G.Loken³⁴, A.Lopez-Fernandez⁷, M.A.Lopez Aguera⁴¹, M.Los³⁰, D.Loukas⁹, J.J.Lozano⁴⁹,
 P.Lutz⁶, L.Lyons³⁴, G.Maehlum¹⁵, J.Maillard⁶, A.Maio²⁰, A.Maltezos⁹, F.Mandl⁵⁰, J.Marco⁴¹, B.Marechal⁴⁷,
 M.Margoni³⁵, J-C.Marin⁷, C.Mariotti⁴⁰, A.Markou⁹, T.Maron⁵², S.Marti⁴⁹, C.Martinez-Rivero⁴¹,
 F.Martinez-Vidal⁴⁹, F.Matorras⁴¹, C.Matteuzzi²⁷, G.Matthiae³⁸, M.Mazzucato³⁵, M.Mc Cubbin²¹, R.Mc Kay¹,
 R.Mc Nulty²¹, J.Medbo⁴⁸, C.Meroni²⁷, W.T.Meyer¹, M.Michelotto³⁵, E.Migliore⁴⁵, I.Mikulec⁵⁰, L.Mirabito²⁴,
 W.A.Mitaroff⁵⁰, G.V.Mitselmakher¹⁴, U.Mjoernmark²³, T.Moa⁴⁴, R.Moeller²⁸, K.Moenig⁷, M.R.Monge¹¹,
 P.Morettini¹¹, H.Mueller¹⁵, W.J.Murray³⁷, B.Muryn¹⁶, G.Myatt³⁴, F.Naraghi¹², F.L.Navarría⁵, P.Negri²⁷,
 S.Nemecek¹⁰, W.Neumann⁵², N.Neumeister⁵⁰, R.Nicolaidou³, B.S.Nielsen²⁸, V.Nikolaenko⁴², P.E.S.Nilsen⁴,
 P.Niss⁴⁴, A.Nomerotski³⁵, A.Normand³⁴, V.Obraztsov⁴², A.G.Olshevski¹⁴, R.Orava¹³, K.Osterberg¹³,
 A.Ouraou³⁹, P.Paganini¹⁸, M.Paganoni²⁷, R.Pain²², H.Palka¹⁶, Th.D.Papadopoulou³¹, L.Pape⁷, F.Parodi¹¹,
 A.Passeri⁴⁰, M.Pegoraro³⁵, J.Pennanen¹³, L.Peralta²⁰, H.Pernegger⁵⁰, M.Pernicka⁵⁰, A.Perrotta⁵, C.Petridou⁴⁶,
 A.Petrolini¹¹, H.T.Phillips³⁷, G.Piana¹¹, F.Pierre³⁹, M.Pimenta²⁰, S.Plaszczynski¹⁸, O.Podobrin¹⁵, M.E.Pol¹⁷,
 G.Polok¹⁶, P.Poropat⁴⁶, V.Pozdniakov¹⁴, M.Prest⁴⁶, P.Privitera³⁸, A.Pullia²⁷, D.Radojicic³⁴, S.Ragazzi²⁷,
 H.Rahmani³¹, J.Rames¹⁰, P.N.Ratoff¹⁹, A.L.Read³², M.Reale⁵², P.Rebecchi¹⁸, N.G.Redaeli²⁷, M.Regler⁵⁰,
 D.Reid⁷, P.B.Renton³⁴, L.K.Resvanis³, F.Richard¹⁸, J.Richardson²¹, J.Ridky¹⁰, G.Rinaudo⁴⁵, A.Romero⁴⁵,
 I.Roncagliolo¹¹, P.Ronchese³⁵, L.Roos¹², E.I.Rosenberg¹, E.Rosso⁷, P.Roudeau¹⁸, T.Rovelli⁵, W.Ruckstuhl³⁰,
 V.Ruhlmann-Kleider³⁹, A.Ruiz⁴¹, K.Rybicki¹⁶, H.Saarikko¹³, Y.Sacquin³⁹, G.Sajot¹², J.Salt⁴⁹, J.Sanchez²⁵,
 M.Sannino¹¹, S.Schael⁷, H.Schneider¹⁵, M.A.E.Schyns⁵², G.Sciolla⁴⁵, F.Scuri⁴⁶, A.M.Segar³⁴, A.Seitz¹⁵,

R.Sekulin³⁷, M.Sessa⁴⁶, R.Seufert¹⁵, R.C.Shellard³⁶, I.Siccama³⁰, P.Siegrist³⁹, S.Simonetti¹¹, F.Simonetto³⁵, A.N.Sisakian¹⁴, G.Skjevling³², G.Smadja²⁴, N.Smirnov⁴², O.Smirnova¹⁴, G.R.Smith³⁷, R.Sosnowski⁵¹, D.Souza-Santos³⁶, T.Spaso²⁰, E.Spiriti⁴⁰, S.Squarcia¹¹, H.Staack⁵², C.Stanescu⁴⁰, S.Stapnes³², I.Stavitski³⁵, G.Stavropoulos⁹, K.Stepaniak⁵¹, F.Stichelbaut⁷, A.Stocchi¹⁸, J.Strauss⁵⁰, J.Straver⁷, R.Strub⁸, B.Stugu⁴, M.Szczekowski⁵¹, M.Szeptycka⁵¹, T.Tabarelli²⁷, O.Tchikilev⁴², G.E.Theodosiou⁹, Z.Thome⁴⁷, A.Tilquin²⁶, J.Timmermans³⁰, V.G.Timofeev¹⁴, L.G.Tkatchev¹⁴, T.Todorov⁸, D.Z.Toet³⁰, A.Tomaradze², B.Tome²⁰, E.Torassa⁴⁵, L.Tortora⁴⁰, G.Transtromer²³, D.Treille⁷, W.Trischuk⁷, G.Tristram⁶, C.Troncon²⁷, A.Tsirou⁷, E.N.Tsyganov¹⁴, M.Turala¹⁶, M-L.Turluer³⁹, T.Tuuva¹³, I.A.Tyapkin²², M.Tyndel³⁷, S.Tzamarias²¹, B.Ueberschaer⁵², S.Ueberschaer⁵², O.Ullaland⁷, V.Uvarov⁴², G.Valenti⁵, E.Vallazza⁷, J.A.Valls Ferrer⁴⁹, C.Vander Velde², G.W.Van Apeldoorn³⁰, P.Van Dam³⁰, M.Van Der Heijden³⁰, W.K.Van Doninck², J.Van Eldik³⁰, P.Vaz⁷, G.Vegni²⁷, L.Ventura³⁵, W.Venus³⁷, F.Verbeure², M.Verlato³⁵, L.S.Vertogradov¹⁴, D.Vilanova³⁹, P.Vincent²⁴, L.Vitale⁴⁶, E.Vlasov⁴², A.S.Vodopyanov¹⁴, M.Vollmer⁵², M.Voutilainen¹³, V.Vrba¹⁰, H.Wahlen⁵², C.Walck⁴⁴, F.Waldner⁴⁶, A.Wehr⁵², M.Weierstall⁵², P.Weilhammer⁷, A.M.Wetherell⁷, J.H.Wickens², M.Wielers¹⁵, G.R.Wilkinson³⁴, W.S.C.Williams³⁴, M.Winter⁸, M.Witek⁷, G.Wormser¹⁸, K.Woschnagg⁴⁸, K.Yip³⁴, O.Yushchenko⁴², A.Zaitsev⁴², A.Zalewska¹⁶, P.Zalewski⁵¹, D.Zavrtanik⁴³, E.Zevgolatakos⁹, N.I.Zimin¹⁴, M.Zito³⁹, D.Zontar⁴³, R.Zuberi³⁴, G.Zumerle³⁵

¹ Ames Laboratory and Department of Physics, Iowa State University, Ames IA 50011, USA

² Physics Department, Univ. Instelling Antwerpen, Universiteitsplein 1, B-2610 Wilrijk, Belgium and IIHE, ULB-VUB, Pleinlaan 2, B-1050 Brussels, Belgium

and Faculté des Sciences, Univ. de l'Etat Mons, Av. Maistriau 19, B-7000 Mons, Belgium

³ Physics Laboratory, University of Athens, Solonos Str. 104, GR-10680 Athens, Greece

⁴ Department of Physics, University of Bergen, Allégaten 55, N-5007 Bergen, Norway

⁵ Dipartimento di Fisica, Università di Bologna and INFN, Via Irnerio 46, I-40126 Bologna, Italy

⁶ Collège de France, Lab. de Physique Corpusculaire, IN2P3-CNRS, F-75231 Paris Cedex 05, France

⁷ CERN, CH-1211 Geneva 23, Switzerland

⁸ Centre de Recherche Nucléaire, IN2P3 - CNRS/ULP - BP20, F-67037 Strasbourg Cedex, France

⁹ Institute of Nuclear Physics, N.C.S.R. Demokritos, P.O. Box 60228, GR-15310 Athens, Greece

¹⁰ FZU, Inst. of Physics of the C.A.S. High Energy Physics Division, Na Slovance 2, CS-180 40, Praha 8, Czechoslovakia

¹¹ Dipartimento di Fisica, Università di Genova and INFN, Via Dodecaneso 33, I-16146 Genova, Italy

¹² Institut des Sciences Nucléaires, IN2P3-CNRS, Université de Grenoble 1, F-38026 Grenoble, France

¹³ Research Institute for High Energy Physics, SEFT, P.O. Box 9, FIN-00014 University of Helsinki, Finland

¹⁴ Joint Institute for Nuclear Research, Dubna, Head Post Office, P.O. Box 79, 101 000 Moscow, Russian Federation

¹⁵ Institut für Experimentelle Kernphysik, Universität Karlsruhe, Postfach 6980, D-76128 Karlsruhe, Germany

¹⁶ High Energy Physics Laboratory, Institute of Nuclear Physics, Ul. Kawioro 26a, PL-30055 Krakow 30, Poland

¹⁷ Centro Brasileiro de Pesquisas Físicas, rua Xavier Sigaud 150, RJ-22290 Rio de Janeiro, Brazil

¹⁸ Université de Paris-Sud, Lab. de l'Accélérateur Linéaire, IN2P3-CNRS, Bat 200, F-91405 Orsay, France

¹⁹ School of Physics and Materials, University of Lancaster, Lancaster LA1 4YB, UK

²⁰ LIP, IST, FCUL - Av. Elias Garcia, 14-1º, P-1000 Lisboa Codex, Portugal

²¹ Department of Physics, University of Liverpool, P.O. Box 147, Liverpool L69 3BX, UK

²² LPNHE, IN2P3-CNRS, Universités Paris VI et VII, Tour 33 (RdC), 4 place Jussieu, F-75252 Paris Cedex 05, France

²³ Department of Physics, University of Lund, Sölvegatan 14, S-22363 Lund, Sweden

²⁴ Université Claude Bernard de Lyon, IPNL, IN2P3-CNRS, F-69622 Villeurbanne Cedex, France

²⁵ Universidad Complutense, Avda. Complutense s/n, E-28040 Madrid, Spain

²⁶ Univ. d'Aix - Marseille II - CPP, IN2P3-CNRS, F-13288 Marseille Cedex 09, France

²⁷ Dipartimento di Fisica, Università di Milano and INFN, Via Celoria 16, I-20133 Milan, Italy

²⁸ Niels Bohr Institute, Blegdamsvej 17, DK-2100 Copenhagen 0, Denmark

²⁹ NC, Nuclear Centre of MFF, Charles University, Areal MFF, V Holesovickach 2, CS-180 00, Praha 8, Czechoslovakia

³⁰ NIKHEF-H, Postbus 41882, NL-1009 DB Amsterdam, The Netherlands

³¹ National Technical University, Physics Department, Zografou Campus, GR-15773 Athens, Greece

³² Physics Department, University of Oslo, Blindern, N-1000 Oslo 3, Norway

³³ Dpto. Fisica, Univ. Oviedo, C/P.Jimenez Casas, S/N-33006 Oviedo, Spain

³⁴ Department of Physics, University of Oxford, Keble Road, Oxford OX1 3RH, UK

³⁵ Dipartimento di Fisica, Università di Padova and INFN, Via Marzolo 8, I-35131 Padua, Italy

³⁶ Depto. de Fisica, Pontificia Univ. Católica, C.P. 38071 RJ-22453 Rio de Janeiro, Brazil

³⁷ Rutherford Appleton Laboratory, Chilton, Didcot OX11 0QX, UK

³⁸ Dipartimento di Fisica, Università di Roma II and INFN, Tor Vergata, I-00173 Rome, Italy

³⁹ Centre d'Etude de Saclay, DSM/DAPNIA, F-91191 Gif-sur-Yvette Cedex, France

⁴⁰ Istituto Superiore di Sanità, Ist. Naz. di Fisica Nucl. (INFN), Viale Regina Elena 299, I-00161 Rome, Italy

⁴¹ C.E.A.F.M., C.S.I.C. - Univ. Cantabria, Avda. los Castros, S/N-39006 Santander, Spain

⁴² Inst. for High Energy Physics, Serpukov P.O. Box 35, Protvino, (Moscow Region), Russian Federation

⁴³ J. Stefan Institute and Department of Physics, University of Ljubljana, Jamova 39, SI-61000 Ljubljana, Slovenia

⁴⁴ Fysikum, Stockholm University, Box 6730, S-113 85 Stockholm, Sweden

⁴⁵ Dipartimento di Fisica Sperimentale, Università di Torino and INFN, Via P. Giuria 1, I-10125 Turin, Italy

⁴⁶ Dipartimento di Fisica, Università di Trieste and INFN, Via A. Valerio 2, I-34127 Trieste, Italy

and Istituto di Fisica, Università di Udine, I-33100 Udine, Italy

⁴⁷ Univ. Federal do Rio de Janeiro, C.P. 68528 Cidade Univ., Ilha do Fundão BR-21945-970 Rio de Janeiro, Brazil

⁴⁸ Department of Radiation Sciences, University of Uppsala, P.O. Box 535, S-751 21 Uppsala, Sweden

⁴⁹ IFIC, Valencia-CSIC, and D.F.A.M.N., U. de Valencia, Avda. Dr. Moliner 50, E-46100 Burjassot (Valencia), Spain

⁵⁰ Institut für Hochenergiephysik, Österr. Akad. d. Wissensch., Nikolsdorfergasse 18, A-1050 Vienna, Austria

⁵¹ Inst. Nuclear Studies and University of Warsaw, Ul. Hoza 69, PL-00681 Warsaw, Poland

⁵² Fachbereich Physik, University of Wuppertal, Postfach 100 127, D-42097 Wuppertal 1, Germany

1 Introduction

The B^0 and \bar{B}^0 mix through box diagrams made possible by second order weak interactions. The oscillation frequency is expressed by the parameter $x_q = \Delta m_q/\Gamma$, where Δm_q is calculated from the diagrams with $q = d, s$. The top quark exchange dominates the process giving the expression for Δm_q :

$$\Delta m_q = \frac{G_F^2}{6\pi} m_B m_t^2 F\left(\frac{m_t^2}{m_W^2}\right) B_B f_B^2 \eta_{QCD} |V_{tb}^* V_{tq}|^2.$$

This relation can be used to determine V_{tq} if the top mass and the hadronic part of the B meson (which is calculable), $B_B f_B^2 \eta_{QCD}$ (where f_B is the decay constant and B_B the 'bag' factor) are known well enough. The dependence on m_t cancels if one considers the ratio x_s/x_d and the hadronic terms for B_s and B_d are expected to be similar; therefore the mixing measurement can give information on the Cabibbo-Kobayashi-Maskawa matrix elements. Time dependent measurements yielding x_d have been performed at LEP [1].

This letter presents a measurement of the time integrated probability of mixing, $\chi = x^2/(2 + 2x^2)$: it is relevant for correcting the measured forward-backward asymmetry of the $b\bar{b}$ final state.

Several measurements of the $B^0 - \bar{B}^0$ mixing parameter χ have already been reported at $p - \bar{p}$ colliders [2] and at e^+e^- machines [3]. In previous DELPHI publications $B^0 - \bar{B}^0$ mixing was measured using the average jet charge [4] and like-sign dilepton events [5]. As already stressed in [4,5], the value of χ accessible to measurement at LEP with those methods is an average value which is a combination of χ_s and χ_d .

This letter presents an update of that measurement based on increased statistics and two different methods to tag the initial flavour. The first is the already standard method of using leptons from the semileptonic decays of b quarks and observing the events with two leptons. The second method consists of tagging one b quark through its semileptonic decay and looking for a Λ ($\bar{\Lambda}$) on the opposite side of the event. The Λ ($\bar{\Lambda}$) unambiguously flags the flavour of the b (\bar{b}) quark whenever it originates from the direct decay of a b -hadron. The result from this method is however at present severely limited by the statistics available and the systematic uncertainties. On the other hand, it is worthwhile to describe it in this letter, mainly to point out a possible new method. Since the selected samples used in the two methods are independent and the measurements can be combined. Both measurements yield $\chi = f_s \chi_s + f_d \chi_d$ where f_s and f_d are the fractions of B_s and B_d produced in the b fragmentation, weighted by the respective semileptonic branching ratios.

2 The DELPHI Detector

The DELPHI detector is described in ref. [6].

The components relevant for this analysis are the tracking chambers, the barrel electromagnetic calorimeter, and the muon chambers. The central tracking includes the vertex detector (VD), the inner detector (ID), the time projection chamber (TPC) and the outer detector (OD). In the forward region the tracking is provided by a system of two drift chambers (FCA and FCB) following the TPC.

The barrel electromagnetic calorimeter (HPC) covers the polar region $45^\circ < \theta < 135^\circ$, and provides the electron identification which is performed only in this angular region.

The geometrical acceptance of the muon chambers is $9^\circ < \theta < 43^\circ$, $52^\circ < \theta < 128^\circ$ and $137^\circ < \theta < 171^\circ$.

3 Selection of events and lepton identification

Hadronic decays, $Z^0 \rightarrow q\bar{q}$, were selected requiring at least 7 charged particles and a total visible energy (from charged particles detected in the tracking chambers and neutrals detected in the calorimeters) larger than $0.3 \times E_{cm}$, where E_{cm} is the centre of mass energy. Tracks were accepted if they had an impact parameter to the nominal interaction vertex below 5 cm in the transverse plane with respect to the beam axis and below 10 cm along the beam direction. Charged particles were required to have momenta greater than 200 MeV/c. Both charged and neutral particles were used in the event reconstruction. A neutral particle was accepted if the energy deposited in the electromagnetic calorimeter was larger than 0.7 GeV and the particle started showering in the first 4.5 radiation lengths when it was inside the HPC. The selection of hadronic Z^0 decays yielded about 207000 events from the 1991 data sample, and about 700000 from 1992.

Muon identification was based on an algorithm using a chi-squared fit, calculated from the difference between the extrapolated track and the track element constructed with the hits in the muon chambers. The algorithm is described in detail in ref. [7].

Electron identification was performed only in the barrel region ($45^\circ < \theta < 135^\circ$), using an algorithm combining the information from the electromagnetic calorimeter HPC (deposited energy, longitudinal shape of the shower) and the dE/dx measurement from the TPC. A V^0 search was applied to reject electron candidates coming from converted photons. Despite that, a Monte Carlo simulation indicates that $(9.7 \pm 0.2)\%$ of identified electrons in the final sample come from unrecognized photon conversions.

Both muons and electrons were selected with restricted criteria to enhance the purity of the sample used. A minimum momentum of 3 GeV/c was required for the lepton to be accepted.

Using these algorithms, the identification efficiencies for electrons and muons within the accepted geometrical and kinematic regions were found to be $(65 \pm 3)\%$ (measured from a sample of Compton electrons selected in the data), and $(76 \pm 1)\%$ respectively. While for muons the agreement between data and simulation, checked with $Z^0 \rightarrow \mu^+\mu^-$ events was very satisfactory, the efficiency for electrons was found to be about 5 to 10% lower in the data than in a sample of simulated Compton electrons. The efficiency for identifying leptons is, however, not crucial in the measurement of the mixing parameter.

The misidentification probability for a pion to be called lepton was checked with real data, using the K^0 decays, and found to be $P_{had \rightarrow \mu} = (0.7 \pm 0.1)\%$ for muons, in good agreement with Monte Carlo predictions. For electrons, a rescaling was necessary, because the simulation overestimated the number of hadrons mimicking electrons inside the HPC. After having applied the rescaling, the misidentification probability $P_{had \rightarrow e}$ was $(0.6 \pm 0.2)\%$.

4 Data and Monte Carlo sample

The final data sample consisted of 5182 events (2349 $\mu\mu$, 658 ee and 2175 $e\mu$) having two leptons in opposite hemispheres with respect to a plane perpendicular to the thrust axis. Of these, 1116 events were collected during 1991, and 4066 during 1992. The number of events with two leptons having the same charge was 2177.

Two samples of Monte Carlo generated $Z^0 \rightarrow q\bar{q}$ decays, corresponding to the 1991 and 1992 detector setups, were used for the analysis. The events were generated with the Lund Parton Shower (PS) model in the JETSET 7.3 program [8], passed through the full detector simulation and processed with the same event reconstruction as the data.

Applying the same selection criteria used for the data gave 14378 dileptons from which the composition of the sample was estimated.

The total statistics of simulated $Z^0 \rightarrow q\bar{q}$ decays were about 530,000 for 1991 and 1,700,000 for 1992.

The heavy quark fragmentation process was described using the Peterson fragmentation function [9] with parameters $\epsilon_b=0.006$ and $\epsilon_c=0.054$. The branching ratios were set to 10.2% for $b \rightarrow \ell$ and 9% for $c \rightarrow \bar{\ell}$. About 1.0 % of b decays occurred through the channel $b \rightarrow \bar{c} \rightarrow \ell$ and about 0.5 % through $b \rightarrow \tau \rightarrow \ell$.

In the analysis however, the branching ratios $b \rightarrow \ell$ and $b \rightarrow c \rightarrow \bar{\ell}$ were rescaled to the values measured from the LEP experiments [10,11], averaging those experiments measuring the branching ratios in the context of the ACCMM semileptonic decay model [12] with parameters as determined in [13]. The averaged values used were $\text{Br}(b \rightarrow \ell) = (11.0 \pm 0.4)\%$ and $\text{Br}(b \rightarrow c \rightarrow \bar{\ell}) = (8.1 \pm 0.4)\%$. The mixing probability measured in the present paper is given in the context of the ACCMM model.

5 Method 1: $B^0 - \bar{B}^0$ mixing with dilepton events

The first method presented here used events with two identified leptons as in ref. [5]. Each lepton in the Monte Carlo sample was assigned, according to its origin, to one of the following classes:

- *PB* (Primary b) : $b \rightarrow \ell$ (including $b \rightarrow \tau \rightarrow \ell$)
- *SC* (Secondary c): $b \rightarrow c \rightarrow \bar{\ell}$
- *S \bar{C}* (Secondary \bar{c}): $b \rightarrow \bar{c} \rightarrow \ell$
- *PC* (Primary c) : $c \rightarrow \bar{\ell}$
- *BCK* : hadrons misidentified as leptons, μ from π and K decays, electrons from converted γ 's or Dalitz decays, leptons from ψ .

Background to the muon sample originated from punch through hadrons, misassociations of hits in the muon chambers, and hadron decays. For electrons, background was generated by γ conversions (the material in front of the HPC calorimeter corresponded to an average of 0.7 radiation lengths, of which 0.2 was before the TPC), and misidentified hadrons.

Each simulated dilepton event was then classified in a combination of two of the previous categories. The sensitivity to the mixing parameter in dilepton events is different for the various categories: for the classes (*PB, PB*), (*SC, SC*), (*PB, S \bar{C}*) the fraction of same sign dileptons is $2\chi(1-\chi)$, while for the classes (*PB, SC*), (*SC, S \bar{C}*) it is the fraction of opposite sign dileptons which has this dependence. The class (*PC, PC*) contributes only to the opposite charge configuration.

Possible biases in the measurement due to correlations in the background class were investigated with simulation. The most important background came from the category (*PB, BCK*) (17% of the total dilepton sample), where BCK is a misidentified hadron. In a sizable fraction of cases (54% of kaons and 22% of pions with $p_t > 1$ GeV/c) the hadron came from the b-hadron and had the right charge, therefore it was correlated with the charge of the lepton of the opposite jet in the same way as in the (*PB, PB*) category. The correlation was parameterized as a function of the variable used in the analysis (p_t defined below), and the pertinent fraction of background was treated as part of the (*PB, PB*) category. The assignment of the non-correlated fraction of the background to the same or opposite charge configuration was taken from the simulation.

In each event, a cluster analysis was made with the LUND algorithm LUCCLUS [8] using both charged and neutral particles and a cutoff parameter $d_{join} = 2.5$ GeV. The transverse momentum, p_t , of a lepton was defined as the momentum component transverse to the rest of the cluster to which the lepton belonged, after the lepton itself had been removed from the cluster. If three or more leptons were found in the event, the two with highest p_t were considered in the analysis. The semileptonic b decays are expected to produce leptons with high p and p_t . In fig. 1, the distribution of the lower transverse momentum of the two leptons is shown, together with the expectations from the different sources of dileptons in the Monte Carlo. The simulation predicts the transverse momentum distribution of the lepton candidates quite well.

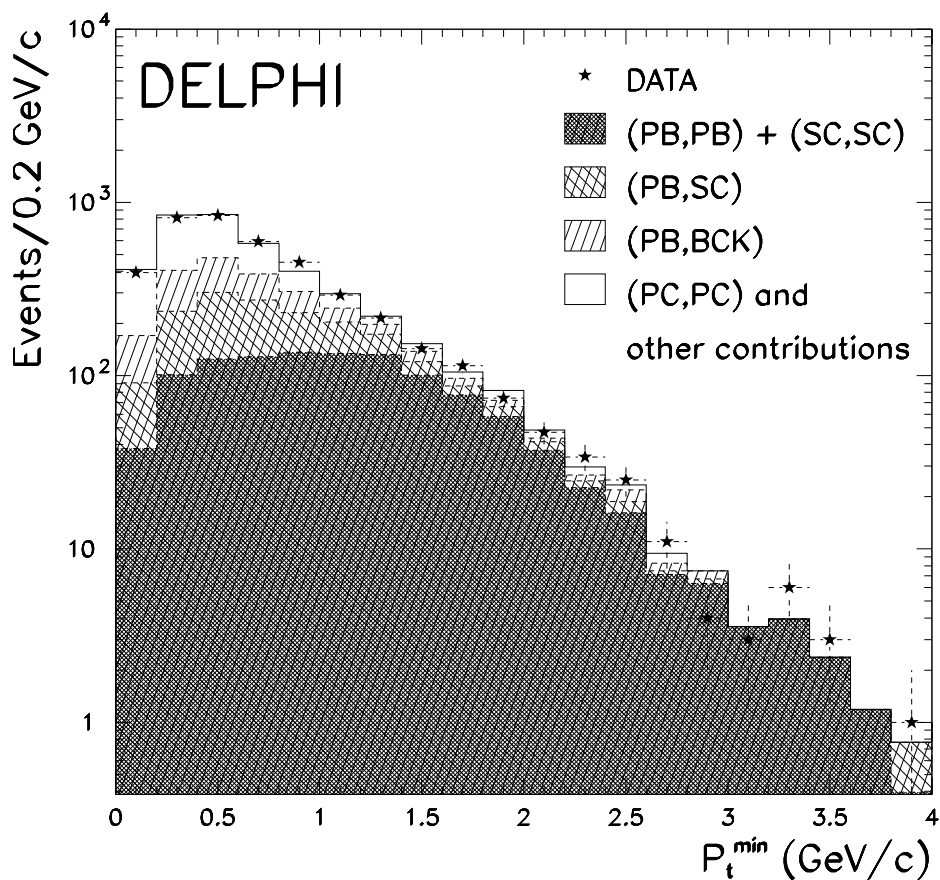


Figure 1: *Dileptons in opposite jets: p_t^{min} distribution for data (stars) and simulation (histograms). The contributions of the different lepton classes are shown.*

The discriminating power of several variables [†] was studied in order to try to enhance the signal to background ratio. These variables were all found to have similar discriminating power and so the simplest variable, the smaller of the p_t values of the two leptons (p_t^{min}), was used.

[†] Variables like e.g. $(\mathbf{p}_1 \times \mathbf{p}_2)$, p_{comb}^{min} , $(p_{t1} \times p_{t2})$, $(p_{t1} + p_{t2})$.

In fig. 2 the contributions from (PB, PB) and (PB, SC) are shown as a function of p_t^{min} . The data in the region where (PB, PB) dominates determine the final measurement of χ .

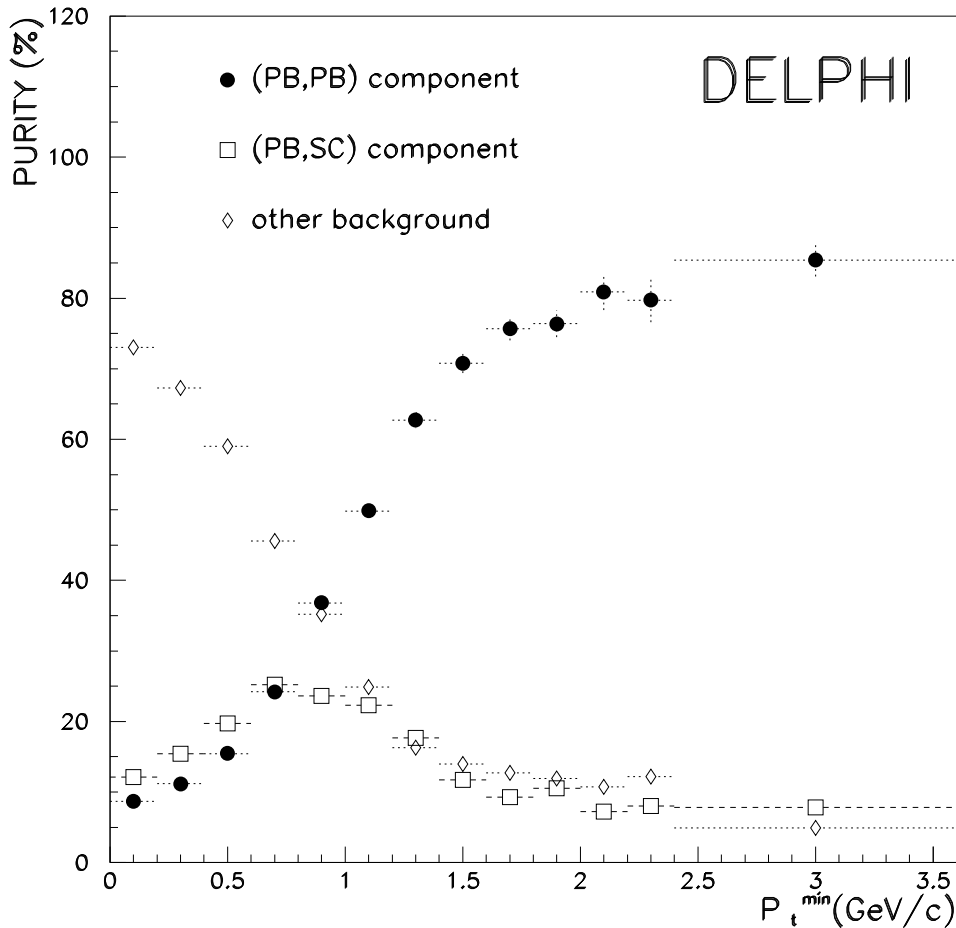


Figure 2: *Dilepton sample composition from the Monte Carlo simulation as a function of the variable p_t^{min} . The contribution (PB, SC) is shown separately: this component dilutes the χ sensitivity.*

The full data sample was used to calculate the fraction of like sign dileptons

$$R_{\ell\ell} = \frac{(\ell^-\ell^-) + (\ell^+\ell^+)}{(\text{all dileptons})}$$

as a function of p_t^{min} . This distribution was compared with that predicted by the simulation as a function of χ , and the χ value determined using a chi-squared fit or a binomial likelihood method.

The branching ratios for $b \rightarrow \ell$ and $b \rightarrow c \rightarrow \bar{\ell}$ of the simulation were rescaled to the values measured by the LEP experiments [10,11] as described at the end of section 4.

The chi-squared fit has the advantage that the error due to the limited Monte Carlo statistics is correctly and straightforwardly taken into account, and it appears convoluted

with the statistical error in the χ value. With the available statistics, the content of each bin was kept above 10 events.

The results were:

$$\chi = (11.9_{-1.6}^{+1.7})\% \text{ from the chi-squared method}$$

and

$$\chi = (12.0_{-1.5}^{+1.6})\% \text{ from the likelihood method}$$

where the errors are statistical only. Applying the statistical method suggested in ref.[14] to take into account the finite Monte Carlo statistics in the likelihood fit, the result was $\chi = (12.1 \pm 1.6)\%$ and completely in agreement with the chi-squared fit result. Figure 3 shows the result of the fit to R .

Another cross-check was to count same sign dileptons after having applied a hard p_t cut ($p_t > 1.4$ GeV/c) in order to select a substantially pure (PB, PB) sample. The resulting 168 same sign dileptons and 426 opposite sign dileptons gave a value:

$$\chi = (11.7 \pm 1.9)\%$$

The method described in this section, applied to simulated $q\bar{q}$ events generated with $\chi = 13.4\%$ yielded $\chi = (13.8_{-1.2}^{+1.3})\%$ in good agreement with the original value.

5.1 Systematic errors on Method 1

There were several sources of systematic uncertainties intrinsic to the simulation used to estimate the background. The most important ones are shown in Table 1, together with the effects on χ . The variations considered were $\pm 1\sigma$, where σ was the experimental error from the available measurements, calculated combining the statistical and systematic errors. The error from the modelling of the semileptonic decay was not added to the σ considered here. Other sources of systematic errors, like the change in the fraction of correlated background or changing the efficiency of lepton identification, were negligible. The stability of the measurement was checked against the binning, the use of different variables and the changes of the criteria for lepton identification. All the measurements were found to be very consistent. The total systematic uncertainty in the mixing measurement was obtained by adding the contributions in quadrature, taking into account the correlation [10,11] between the branching ratios $\text{Br}(b \rightarrow \ell)$ and $\text{Br}(b \rightarrow c \rightarrow \bar{\ell})$. The resultant systematic error was $(\pm 0.4)\%$. This error is largely dominated by the ratio of the above two branching ratios.

The differences between the models of the semileptonic decay also contributes to the systematic error. The lepton momentum distribution in the rest frame of the B hadron was reweighted according to different decay models. The ACCMM[12] and the IGSW[15] models were considered. The ACCMM model predicts [‡] the inclusive $b \rightarrow \ell$ spectrum, while in the IGSW model the spectrum depends on the relative production rates of D, D* and D**. The IGSW model was adjusted to the fraction of D** ($21 \pm 8\%$) measured from the CLEO data [16]. The variation quoted in table 1 corresponds to $\pm 1\sigma$ of this percentage.

The final result was:

$$\chi = (12.1 \pm 1.6 \pm 0.4(\text{sys.}) \pm 0.4(\text{mod.}))\%$$

[‡]It was checked that the χ value was not significantly affected when the ACCMM parameters values changed from the ones in [10].

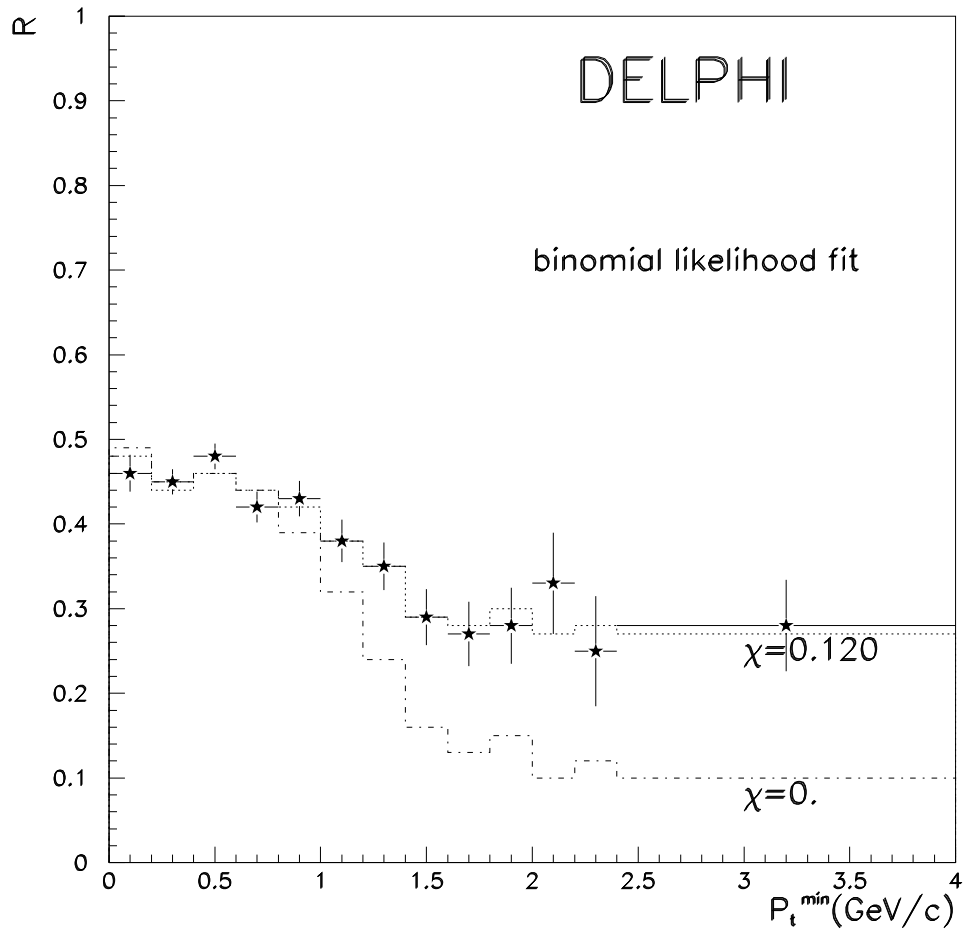


Figure 3: Ratio $R_{\ell\ell}$ as a function of p_t^{min} together with the fitted values corresponding to $\chi = 12.0\%$. Also shown are the values corresponding to $\chi = 0$.

Source	Relative variation	Effect on χ
$\text{Br}(b \rightarrow \ell)$	$\pm 4\%$	
$\text{Br}(b \rightarrow c \rightarrow \bar{\ell})$	$\pm 5\%$	$\mp 0.4\%$
$\text{Br}(b \rightarrow \bar{c} \rightarrow \ell)$	$\pm 50\%$	$< 0.05\%$
$\text{Br}(b \rightarrow \tau)[17]$	$\pm 23\%$	$< 0.05\%$
$\text{Br}(c \rightarrow \bar{\ell})$	$\pm 10\%$	$< 0.05\%$
Hadron misidentification	$\pm 10\%$	$< 0.05\%$
Fragmentation function	$\epsilon_b = 0.005 - 0.007$	$\pm 0.1\%$
Total		0.4%
Semileptonic decay model	IGSW with $(21 \pm 8)\% D^{**}$	$\pm 0.4\%$

Table 1: Contributions to the systematic uncertainty in the measurement of the mixing parameter. Variations given in percent are relative to the values in the simulation.

6 Method 2: Mixing with $\Lambda\ell^\pm$ events

Final state Λ and $\bar{\Lambda}$ baryons originating from the cascade decay of b -hadrons through charmed baryons are of interest because they flag the flavour of the original b -quark, in the same way as the charge of the leptons from the semileptonic decay of b -hadrons does. Thus the set of $b\bar{b}$ events where one b -hadron decays semileptonically and the other cascades to a Λ baryon in the opposite hemisphere can be used to tag the initial sample to study $B^0 - \bar{B}^0$ mixing. Once the sign combinations of the baryon and lepton number are considered, the presence of a like sign $\Lambda\ell$ pair ($\Lambda\ell^-$ or $\bar{\Lambda}\ell^+$) is the signature of mixing, while an opposite sign pair ($\Lambda\ell^+$ or $\bar{\Lambda}\ell^-$) indicates that mixing did not occur. The dependence of the fraction of like sign $\Lambda\ell$ pairs on the mixing parameter χ for $b\bar{b}$ events is given by:

$$R = \frac{\Lambda\ell^- + \bar{\Lambda}\ell^+}{\Lambda\ell + \bar{\Lambda}\ell} = 2\chi(1 - \chi)A + \chi(1 - A) \quad (1)$$

where

$$A = \frac{BR(B \rightarrow \Lambda)}{BR(B \rightarrow \Lambda)(1 - f_{b\text{-baryons}}) + f_{b\text{-baryons}}BR(b\text{-baryon} \rightarrow \Lambda)} \quad (2)$$

and $f_{b\text{-baryons}}$ is the fraction of b -baryons. The parameter A takes into account the fact that B mesons can undergo baryonic decays but with different branching ratios from b -baryons. The baryonic decay of B mesons to Λ has been measured by CLEO [18] to be $BR(B \rightarrow \Lambda) = (3.8 \pm 0.7)\%$.

The LEP experiments have measured the product of the b -baryon production fraction and semileptonic branching ratio to a final state including a Λ , $f_{b\text{-baryons}}BR(b\text{-baryon} \rightarrow \Lambda\ell^- X)$ [19]. Assuming the Standard Model $\Gamma_{b\bar{b}}$ value and taking into account the common systematic error, the combined measurement value is $f_{b\text{-baryons}}BR(b\text{-baryon} \rightarrow$

$\Lambda \ell^- X) = (0.31 \pm 0.08)\%$. The Λ production in b-baryon decays has been extracted from it assuming a semileptonic branching ratio common to all the b-hadrons; systematics due to this hypothesis have been taken into account allowing a $\pm 10\%$ variation of the semileptonic branching ratio of b-baryons with respect to the measured value, averaged over the b-hadron species. The b-baryon fraction $f_{b\text{-baryons}}$ can also be extracted, following the OPAL analysis [19], assuming $Br(b\text{-baryon} \rightarrow \Lambda_c) = (80 \pm 20)\%$, and $Br(\Lambda_c \rightarrow \Lambda) = (45 \pm 15)\%$ as measured by CLEO [18]. The estimated value is $f_{b\text{-baryons}} = (7.8_{-3.9}^{+5.2})\%$, where the systematic errors on the branching ratios have also been taken into account. Using the above results the value of the parameter A was calculated to be $A = 0.60 \pm 0.07$.

The mixing signature in the sample is diluted by the background and the experimentally measured fraction of like sign pairs does not correspond directly to $R_{PB,PB}$. Possible sources of leptons have been already summarized in section 5; Λ candidates are assumed to be produced only by:

- b-hadron cascade decay (PB)
- primary c baryon decays (PC)
- hadronization and combinatorial background in the Λ mass region (BKG).

Defining $q_{i,j}$ as the fraction of pairs coming from the Λ source i and the lepton source j and $R_{i,j}$ as the corresponding ratio of like sign pairs over the sum of opposite and like sign pairs, the measured value of the ratio may be parameterized as

$$R_{meas} = R_{PB,PB} q_{PB,PB} + R_{PB,S\bar{C}} q_{PB,S\bar{C}} + R_{PB,SC} q_{PB,SC} + R_{PC,PC} q_{PC,PC} + R_{BKG} q_{BKG} \quad (3)$$

The ratio $R_{PB,PB}$ has been defined in equation 1. Assuming that whenever the Λ and/or the lepton comes from the background like and unlike pairs are produced equally results in $R_{BKG} = 0.5$; with $R_{PC,PC} = 1$, $R_{PB,S\bar{C}} = R_{PB,PB}$ and taking into account the χ dependence of $R_{PB,SC}$, equation 3 may be written in suitable form for extracting the mixing parameters:

$$R_{meas} = a \chi - b \chi^2 + c \quad \text{where} \quad \begin{cases} a = (1 + A) (q_{PB,PB} - q_{PB,SC} + q_{PB,S\bar{C}}) \\ b = 2 A (q_{PB,PB} - q_{PB,SC} + q_{PB,S\bar{C}}) \\ c = q_{PB,SC} + q_{PC,PC} + 0.5 q_{BKG} \end{cases} \quad (4)$$

6.1 Results from method 2

The result presented here is from the 1991 and 1992 data taking periods. The Λ selection criteria were studied and the cuts were optimized for this analysis. The $\Lambda \rightarrow \pi p$ candidate was required to fulfill the following:

- Good secondary vertex reconstruction probability (chi-squared probability larger than 1%);
- Collinearity between the line of flight of the Λ and its reconstructed momentum;
- The dE/dx measured in the TPC for the proton (defined as the higher momentum particle) consistent with the proton hypothesis and similarly the dE/dx of the other particle consistent with the pion hypothesis;
- Rejection of reflection from K^0 decays and from γ 's converted in the detector.

<i>EventType</i>	<i>Total(%)</i>
<i>PB, PB</i>	37.8 ± 2.2
<i>PB, S\bar{C}</i>	0.6 ± 0.1
<i>PB, SC</i>	4.5 ± 0.9
<i>PC, PC</i>	5.2 ± 1.2
<i>BKG</i>	51.9 ± 2.3

Table 2: *Sample composition after the selection cuts, estimated from the full DELPHI simulation. The percentage of each event class corresponds to the $q_{i,j}$ coefficients in equation 4.*

The information from the RICH detector, whenever available, was used to confirm that the higher momentum particle was a proton and not a pion. The average reconstruction efficiency after all the cuts was found to be 17% for Λ momenta larger than 4 GeV/c. In order to enhance the (PB,PB) purity in the $\Lambda\ell$ sample, kinematic cuts were applied on both the Λ and the lepton candidates. The contribution from SC and PC decays was suppressed by requiring that the lepton has transverse momentum (p_t) of at least 1 GeV/c with respect to the axis of the closest hadronic jet. The requirement for high lepton momentum (greater than 3 GeV/c) reduces the hadron misidentification probability. Setting a 5 GeV/c lower threshold on the Λ momentum strongly reduces the background from Λ produced in the hadronization process.

Fig.4 shows the invariant mass spectra for Λ candidates belonging to opposite and like sign $\Lambda\ell$ pairs which satisfy the event selection criteria. The signal was integrated over the region 1.106 - 1.126 GeV/c² giving a final sample of 162 opposite sign $\Lambda\ell$ pairs and 117 like sign pairs.

The value of R_{meas} obtained is:

$$R_{meas} = 0.419 \pm 0.030 \quad (5)$$

The sample composition has been determined applying the same reconstruction method and selection criteria to events simulated in the complete detector. The combinatorial background underneath the Λ peak in the simulation has been scaled to match the data and the error on the scaling factor has been taken into account; the cross section for Λ produced during the fragmentation process has been scaled to the latest published measurements [20].

Relying on the sample composition shown in table 2, the mixing parameter value can be extracted from R_{meas} via equation 4:

$$\chi = (12.9^{+7.5}_{-6.5}) \% \quad (6)$$

where the error is only statistical.

6.2 Systematic Errors on Method 2

The main systematic uncertainties affecting the measurement are due to the errors in the measured branching fractions appearing in equation 4 and to the limited statistics

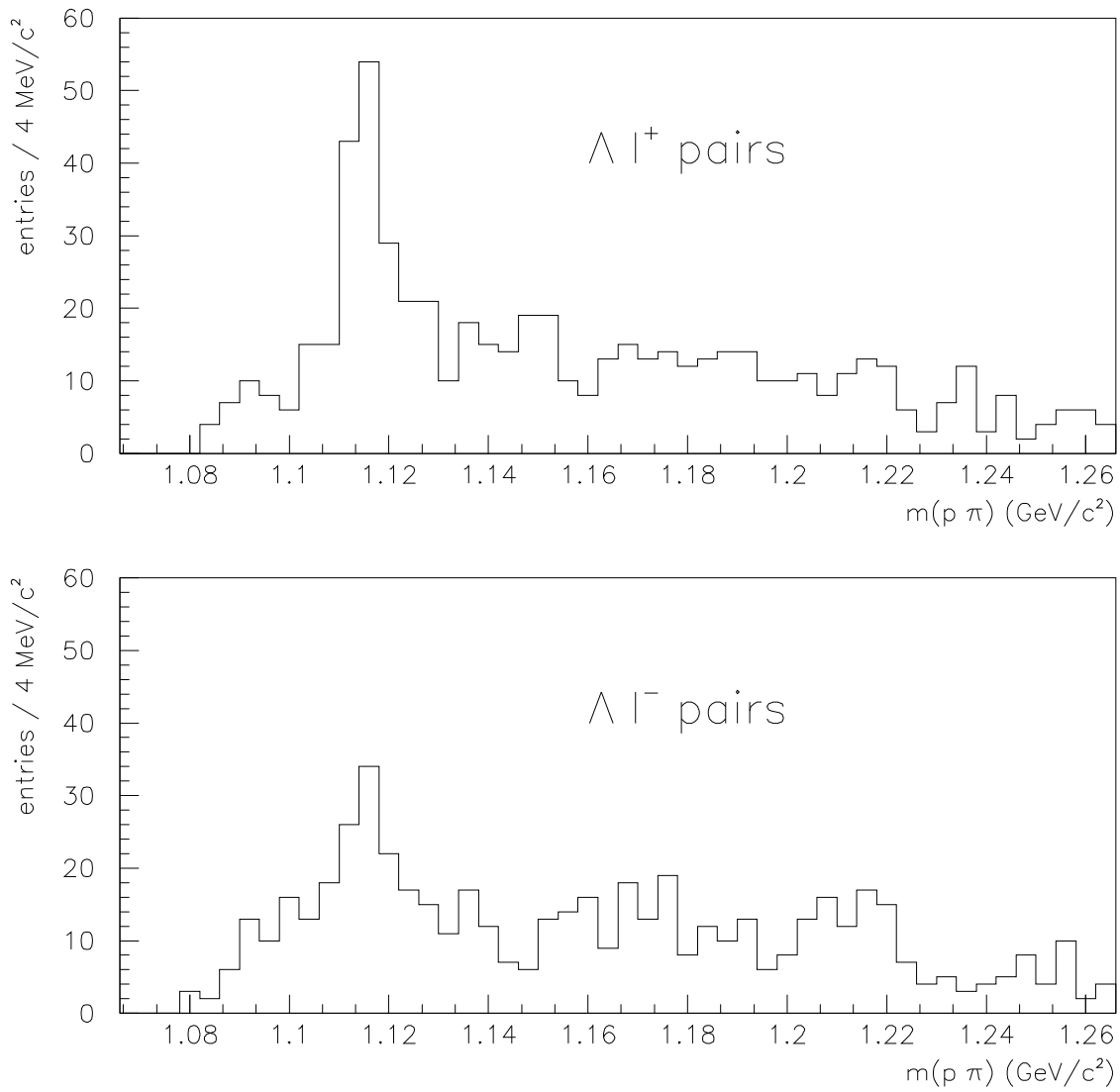


Figure 4: $p\pi$ invariant mass distribution for Λ candidates correlated to either a negative or a positive lepton. Charge conjugated correlations are implied

of the simulation used to estimate the sample composition. The effect of the former is summarized in table 3. The latter, corresponding to the sample composition uncertainties shown in table 2, induces a $\pm 2.5\%$ error. Uncertainties on the background contribution arising from the disagreement between the data and the simulation as well as uncertainties on the Λ production cross section and the lepton purity add a further $\pm 0.4\%$ error. Taking all systematic errors into account the measured mixing parameter value was:

$$\chi = (12.9_{-6.5}^{+7.5} (stat) \pm 3.6(syst) \pm 2.5(MCstat))\% \quad (7)$$

Source	Variation	Effect on χ
$Br(b - baryon \rightarrow \Lambda_c)$	$\pm 20\%$	$\pm 0.2\%$
$f_{b-baryons} Br(b - baryon \rightarrow \Lambda \ell)$	$\pm 25\%$	$\pm 2.1\%$
$Br(bbaryon \rightarrow \ell X)$	$\pm 10\%$	$\pm 0.7\%$
$Br(B \rightarrow \Lambda)$	$\pm 18\%$	$\pm 1.3\%$
$Br(\Lambda_c \rightarrow \Lambda)$	$\pm 33\%$	$\pm 2.2\%$
$Br(b \rightarrow \ell)$	$\pm 4\%$	$\pm 0.2\%$
$Br(c \rightarrow \bar{\ell})$	$\pm 10\%$	$\pm 0.8\%$
$Br(b \rightarrow c \rightarrow \bar{\ell})$	$\pm 5\%$	$\pm 0.2\%$
$Br(b \rightarrow \bar{c} \rightarrow \ell)$	$\pm 50\%$	$\pm 0.5\%$
Total		$\pm 3.6\%$

Table 3: *Systematic error in the measurement of the mixing parameter χ from branching ratio uncertainties. Variations are relative to the values used in the simulation.*

7 Conclusions

Using a total sample of 5182 dilepton events, containing both muons and electrons, the average $B^0 - \bar{B}^0$ mixing parameter in the Z^0 decays has been found to be:

$$\chi = (12.1 \pm 1.6(stat) \pm 0.4(syst) \pm 0.4(model))\%$$

A sample of 279 $\ell\Lambda$ events with $p_t > 1\text{GeV}/c$ yielded:

$$\chi = (12.9_{-6.5}^{+7.5} (stat) \pm 3.6(syst) \pm 2.5(MCstat))\% \quad (8)$$

The combined result is :

$$\chi = (12.1 \pm 1.6 \pm 0.4 \pm 0.4)\%$$

where the last 0.4 is the error due to the model of semileptonic decay. The final result is dominated completely by the more precise measurement with the dilepton sample.

The measurement presented here can be combined with the published DELPHI result based on the average charge of jets correlated to a lepton with high p_t [4]. To do so,

one has to take into account the statistical correlation due to the fact that the data samples used in the present analysis are included in the sample used in ref.[4] and that the measured χ corresponds to a different combination of χ_d and χ_s . The combined result is

$$\bar{\chi} = f_d\chi_d + 0.96f_s\chi_s = (13.1 \pm 1.4)\%$$

where the error includes the statistical and systematic uncertainties. The coefficient 0.96 is determined by the weights in the combination of the two different definitions of χ in [4] and in the present paper.

Acknowledgements

We are greatly indebted to our technical collaborators and to the funding agencies for their support in building and operating the DELPHI detector, and to the members of the CERN-SL Division for the excellent performance of the LEP collider.

References

- [1] ALEPH Coll., D.Decamp et al, *Phys. Lett.* **B 313** (1993) 498.
ALEPH Coll., D. Buskulic *et al.*, CERN-PPE/93-221 .
OPAL Coll., R.Akers *et al.*, CERN-PPE/94-43 .
- [2] UA1 Coll., H.C.Albajar *et al.*, *Phys.Lett.* **B 186** (1987) 247
Phys.Lett. **B 262** (1991) 171
F.Abe et al., *Phys. Rev. Lett.* **67** (1991) 3351.
- [3] CLEO Coll., J.Bartelt et al., *Phys.Rev.Lett.* **71** (1993) 1680
ARGUS Coll.,H.Albrecht et al., *Z. Phys.* **C 55** (1992) 357.
ALEPH Coll., D.Decamp et al, *Phys. Lett.* **B 258** (1991) 236.
ALEPH Coll., D.Buskulic et al, *Phys. Lett.* **B 284** (1992) 177.
OPAL Coll.,P.D.Acton. et al., *Phys. Lett.* **B 276** (1992) 379.
L3 Coll., B.Adeva et al., *Phys. Lett.* **B 288** (1992) 395.
- [4] DELPHI Coll., P. Abreu et al., *Phys. lett.* **B 322** (1994) 459.
- [5] DELPHI Coll., P.Abreu, *Phys. Lett.* **B 301** (1993) 145.
- [6] DELPHI Coll., P.Abreu et al., *Nucl. Phys.* **B 367** (1991) 511.
- [7] L. De Boeck, G.R. Wilkinson *DELPHI note* 93-14 PHYS.
- [8] T. Sjöstrand et al., in “*Z physics at LEP 1*”, CERN 89-08, CERN, Geneva, 1989.
*Comp.Phys.Comm.***39** (1986) 347.
- [9] C. Peterson et al., *Phys. Rev.* **D 27** (1983) 105.
- [10] ALEPH Coll., D. Buskulic *et al.*, CERN-PPE/94-17 and *Z.Phys.* **C**.
- [11] OPAL Coll.,R.Akers *et al.*, *Z. Phys.* **C 60** (1993) 199.
- [12] G. Altarelli et al., *Nucl. Phys.* **B 208** (1982) 365.
- [13] CLEO Coll., S. Henderson,*et al.*, *Phys. Rev.* **D 45** (1992) 2212.
- [14] K.Moenig ,*DELPHI Note 93/57 June 1993*
- [15] N. Isgur et al., *Phys.Rev.* **D 39** (1989) 799
- [16] B.Ong et al, *Contributed Paper to XVI International Symposium on LEPTON-PHOTON Interactions, Cornell University, Ithaca, NY 1993.*
- [17] ALEPH Coll., D. Buskulic *et al.*, *Phys. lett.* **B 298** (1993) 479.
- [18] CLEO Coll., G. Crawford *et al.*, *Phys. Rev.* **D 45** (1992) 752.
ARGUS Coll., H.Albrecht *et al.*, *Z. Phys.* **C 56** (1992) 1.
- [19] DELPHI Coll., P. Abreu *et al.*, *Phys. lett.* **B 311** (1993) 379.
ALEPH Coll., D. Buskulic *et al.*, *Phys. lett.* **B 297** (1992) 449.
OPAL Coll., P.D. Acton *et al.*, *Phys. lett.* **B 281** (1992) 394.
- [20] DELPHI Coll., P. Abreu *et al.*, *Phys. lett.* **B 318** (1993) 249.